Development of Rolled Scaffold for high-density adherent cell culture

Ashkan YekrangSafakar[1], Katie M. Hamel[2], Ali Mehrnezhad[1], Jangwook P. Jung[2] and Kidong Park[*1]

[1] Division of Electrical and Computer Engineering, Louisiana State University, Baton Rouge, Louisiana, U.S.A.

[2] Department of Biological Engineering, Louisiana State University, Baton Rouge, Louisiana, U.S.A.

***Corresponding author:**

Kidong Park, Division of Electrical and Computer Engineering, Louisiana State University, Baton Rouge, 70803, LA, U.S.A.
E-mail: kidongp@lsu.edu Phone: 225-578-5336

Abstract

Bioreactors for large-scale culture of mammalian cells are playing vital roles in biotechnology and bioengineering. Various bioreactors have been developed, but their capacity and efficiency are often limited by insufficient mass transfer rate and high shear stress. A rolled scaffold (RS) is a fully defined scaffold for high-density adherent culture of mammalian cells. The RS is a polymer film with spacers, that is rolled into a cylinder with a pre-determined gap between each turn. Cells are cultured on its inner surfaces, while media flows through the gap. The RS exhibits high surface-area-to-volume ratio over 100 cm^2/mL and can transport nutrients and gases with significantly reduced shear stress via convection in a unidirectional laminar flow, rather than diffusion and random turbulent flow as in stirred-tank bioreactors. In this paper, we expanded Chinese Hamster Ovary cells with RS bioreactors and demonstrated cell culture density over 60 million cells/mL with a growth rate higher than conventional suspension culture. Besides, murine embryonic stem cells were successfully expanded without losing their pluripotency. The RS will provide an affordable, scalable, and reliable platform for large-scale culture of recombinant cells in biopharmaceutical industries and shear-sensitive stem cells for tissue engineering.

Keyword: high-density cell culture, anchorage-dependent cells, scaffold, bioreactor, cell expansion

1. Introduction

Biopharmaceutical industry (Walsh 2014; Wurm 2004) uses mammalian cells to produce therapeutic proteins and monoclonal antibodies (Reichert et al. 2005). In tissue engineering and regenerative medicine, billions of stem cells are used to fabricate tissue engineered constructs (Billiet et al. 2014; Yan et al. 2005) or to replenish lost or damaged cells in degenerative diseases (Chong et al. 2014; Shiba et al. 2016). With these various demands in biotechnology, there is a strong and immediate need for a reliable and efficient platform to culture a large amount of mammalian cells.

Various methods have been developed to culture mammalian cells on a large scale. Multilayer flasks (Abraham et al. 2017; Chen et al. 2014) can be used to culture anchorage-dependent cells on a large scale. Scaling up this approach is straightforward from the conventional 2D techniques. However, the maximum culture capacity is limited and the techniques requires manual operation (Jenkins and Farid 2015). Currently, the stirred-tank bioreactor is widely used. Culture medium is sparged with air bubbles and stirred with impellers. This provides a uniform and sufficient level of nutrients and dissolved gases. The cells are suspended in the culture medium either as single cells (Chotteau et al. 2014), cell aggregates (Krawetz et al. 2009; Olmer et al. 2010), or cells attached to microcarriers (Badenes et al. 2016; Gupta et al. 2016). In the biopharmaceutical industry, genetically engineered cells are cultured as suspended single cells to produce recombinant proteins and monoclonal antibodies (Wurm 2004). Stem cells, such as induced pluripotent stem cells (iPSCs) and mesenchymal stem cells (MSCs), are anchorage-dependent and often cultured as cell aggregates (Krawetz et al. 2009; Olmer et al. 2010).

Recently, a number of new platforms are commercialized to facilitate the large-scale culture of mammalian cells. One of the recent developments is a disposable plastic bag on a

rocking platform (Eibl et al. 2009; Singh 1999). This approach is similar to a stirred-tank bioreactor where cells are suspended and the culture medium is mechanically agitated. However, the culture medium is agitated by a gentle rocking motion and the shear stress on the suspended cells is reduced (Eibl et al. 2009). Other commercialized techniques include hollow-fiber bioreactors (Mizukami et al. 2018) and packed-bed bioreactors (Cino et al. 2003; Merten et al. 2001) with porous scaffolds. These platforms typically achieve high cell culture densities and a more favorable microenvironment. However, they still lack the culture capacity and scalability compared to industrial scale stirred-tank bioreactors.

Due to its simple structure, stirred-tank bioreactors are widely used in biopharmaceutical industries (Chu and Robinson 2001). The transport of nutrients and oxygen in stirred-tank bioreactors relies on diffusion and random turbulent flow generated by impellers. As the capacity of the bioreactor increases, the surface-area-to-volume ratio of the culture medium decreases. To maintain sufficient mass transfer rate of nutrients and oxygen in larger stirred-tank bioreactors, the mechanical agitation and sparging should be increased. This will increase hydrodynamic shear stress (Abu-Reesh and Kargi 1991; Oh et al. 1989; Senger and Karim 2003), which can adversely affect cell proliferation or protein production. As such, when scaling up, the mass transfer rate and the hydrodynamic shear stress have to be carefully balanced for optimal culture conditions. The scale and geometry of stirred-tank bioreactors greatly affect both the hydrodynamic shear stress and the mass transfer rate. For this reason, empirical approaches are often used to optimize the expansion protocol of a specific cell line for each bioreactor with different capacity. Also, cell lines commonly used in biopharmaceutical industries have to be adapted to suspension culture over multiple generations and screened for scalability (Sinacore et al. 2000; Wurm 2004). Besides, stem cells such as MSCs and iPSCs are inherently anchorage-dependent and a ROCK inhibitor

(e.g. Y-27362) should be used to maintain initial viability of the suspended single cells (Amit et al. 2010) until they form cell aggregates. In addition, the stirring rate should be even more carefully adjusted in stem cell expansion, as it affects the size of cell aggregates (Moreira et al. 1995; Sen et al. 2002) and differentiation potential (Gareau et al. 2014; Leung et al. 2010; Stolberg and McCloskey 2009; Wolf and Mofrad 2009).

Here we report a novel rolled scaffold (RS) for large-scale adherent culture of anchorage-dependent cells. The RS is a scalable scaffold for high-density adherent culture of mammalian cells. It is fabricated by rolling a thin plastic film with UV-imprinted spacers into a cylinder with a predetermined gap between each turn, as shown in Fig. 1. The cells are attached to and growing on the internal surfaces of the RS, while the culture medium flows through the gap. The RS is unique in that its microarchitecture is fully defined and engineered for optimal transport of oxygen and nutrients. Unlike stirred-tank bioreactors, nutrients and oxygen are transported through convection in a unidirectional laminar flow with higher efficiency. This drastically reduces the hydrodynamic shear stress. More importantly, the capacity of the RS is scaled up by rolling more plastic film with same spacers and the microenvironment is consistent with increasing culture capacity. The current design provides a surface-area-to-volume ratio over 100 cm^2/mL. In this paper, we present the fabrication process and the dimensional analysis of the RS. We demonstrate the expansion of Chinese Hamster Ovary (CHO) cells with a higher growth rate and the successful culture of murine embryonic stem cells (mESCs).

2. Material and Methods

Fabrication of Rolled scaffold: The fabrication process of the RS is presented in Fig. 2a. An array of grooves with 1 mm spacing and 100 μm depth were engraved on a 1.6 mm thick silicon rubber sheet with a laser engraver (VLS 2.30, Universal laser system Inc., USA). After washing the

engraved silicon rubber with water and soap, the grooves were filled with ultraviolet (UV) curable resin (1187-M, Dymax, U.S.A.) and covered with a 50 µm thick polyethylene terephthalate (PET) film. The mold was placed under a 100 W UV LED (light emitting diode) with the peak wavelength of 349 nm for 5 minutes to cure the resin. The film was detached from the mold with the cured UV-resin to form 100 µm high spacers. The mold was cleaned with 70% ethanol for reuse. The film was washed in 70% ethanol for 1 minute to remove the residue of the UV-resin between the spacers. Figure 2b shows the SEM (scanning electron microscope) image of the film with spacers. Afterward, the films were rolled tightly around a Nylon core rod with a diameter of 3.18 mm to form the RS, as shown in Fig. 2c. The diameter of the RS depends on the length of the film. The film length was 34 cm for a small RS and 240 cm for a medium RS. Two syringes with a luer-lock port were cut to make a RS holder, as shown in Fig. 2d. The holder was sealed with the UV-resin on the joint. Two 3 mL syringes (309657, BD, USA) with a 4.75 mm inner radius and two 30 mL syringes (309650, BD, USA) with a 10.75 mm inner radius were used to make holders for a small RS and a medium RS.

Experimental setup: Figure 2e represents a schematic diagram of the setup. Prior to assembly, all of the parts except the RS and the spinner flask were sterilized with 70% ethanol for 15 minutes. RSs and spinner flasks were autoclaved. A 100 ml spinner flask (CLS-1430-100, Chemglass, USA) with 100 ml of culture medium and a 1 L spinner flask (Bellco Glass, Inc., USA) with 1 L of culture medium were used as reservoirs for a small RS and a medium RS. Tubing with a diameter of 1.6 mm was used for fluidic connections. The upstream oxygen sensor (FTC-SU-PSt3 & OXY-1 SMA, PreSens, Germany) measured the dissolved oxygen concentration of the culture medium in the reservoir and the downstream oxygen sensor measured the culture medium passing through the RS. Each access port between the oxygen sensor and the RS consisted of a 3-way stopcock

valve (GH-30600-23, Cole-Parmer, USA) and a needleless aseptic connector (C1000, Clave Connector, ICU Medical, Inc., USA) for aseptic fluid handling. A peristaltic pump (UX-77300-40, Masterflex, USA) was used to circulate the culture medium through the RS while a magnetic stirrer platform (440811, Corning, USA) stirred the medium in the reservoir. Glucose concentration and pH of the medium was measured by a glucose meter (GlucCell^{TM}, Cesco Bioengineering, Taichung, Taiwan) and a pH meter (UX-05662-51 and UX-35618-32, Cole Parmer, USA). Humidified air was injected into the reservoir using a 3 W air pump (AAPA7.8L, Active Aqua, USA). To control and monitor the air pressure in the reservoir, a rotameter (7530-1-1-1-2C-01, King Instrument, USA) and a pressure gauge (PEM199, Winters Instruments, USA) were used.

Cell line and characterization protocols: See supplementary information for details.

Cell seeding and culture: To facilitate the attachment of CHO cells, the RS was filled with poly-L-lysine solution (P4707, Sigma-Aldrich, USA) and incubated for 1 hour at 37 °C, followed by a PBS wash. Similarly, the RS was coated with 0.1% (v/v) solution of gelatin (16566, Electron Microscopy Sciences, USA) for 1 minute to enhance the attachment and growth of mESC. Then, the RS and the tubing were washed with culture medium. The RS was seeded by injecting the cell suspension through the downstream access port, while the RS was kept vertical. Knowing the surface area of the RS and the volume of media that is required to fill its channels, we calculated the seeding density in cell/mL for each cell line. CHO cells were seeded at a density of 10^6 cells/mL to have a target seeding density of 5×10^3 cells/cm^2, at which the CHO cells had been seeded for 2D culture. mESCs were seeded at a density of 8×10^6 cells/mL to have a target seeding density of 4×10^4 cells/cm^2. In a typical 2D cell culture, mESC were seeded at 10^4 - 10^5 cells/cm^2(Jaccard et al. 2014; Kohlmeier et al. 2013; Stoelzle et al. 2011). After seeding, the setup was moved into an incubator with 5% CO_2 at 37 °C and incubated without medium flow for 4 hours to ensure

proper cell attachment, while the RS was kept horizontal. After cell attachment, the media was circulated with the peristaltic pump. The flow rate was doubled when the downstream oxygen concentration became lower than 3 mg/L. To replenish the depleted nutrients, a concentrated nutrient supplement (CHO CD EfficientFeed™ A Nutrient Supplement, Gibco, USA) was added to the reservoir.

Cell harvesting protocol: To harvest the expanded cells, the RS was removed from the setup by disconnecting the 3-way stopcock valves from the oxygen sensors. Through the upstream access port, PBS was injected to wash away the culture medium, followed by the injection of trypsin (25200056, Life Technologies, USA) for CHO cells and accutase (AT104-100ml, Innovative Cell Technologies, Inc., USA) for mESCs. After incubating at 37°C for 4 minutes, the RS was gently washed with fresh culture medium to wash away the detached cell. The cell detachment process was repeated a few times to ensure the complete collection.

3. Result and Discussion

Key characteristics of the RS can be controlled by varying its dimension and the flow rate of the medium. Figure 3a shows the surface area of the RS that is proportional to the square of its radius and inversely proportional to the spacer's height. The surface area, A, can be described as below,

$$A = \frac{2\pi\left(R^2 - r^2\right)L}{h + t} \times 0.9 \qquad (1)$$

where R, r, L, h, and t are radius of the RS, radius of the core rod, length of RS, height of the spacers, and thickness of the PET film, respectively. In this study, h was 100 μm, t was 50 μm, and L was 4.3 cm. The surface area of a small RS with R of 4.5 mm and that of a medium RS with R of 10.75 mm were 251 cm^2 and 1831 cm^2, which were equivalent to 10 and 73 T-25 culture

flasks. The volume of the small RS and the medium RS were 2.5 mL and 16 mL. The surface-area-to-volume ratio of the small RS and the large RS were 100.4 cm^2/mL and 114.4 cm^2/mL, respectively.

The surface-area-to-volume ratio can be increased, by reducing h. However, this will increase the hydrodynamic shear stress on the cells. The shear stress, τ, in the RS can be calculated with the Poiseuille equation (Holt et al. 2006; Longuet-Higgins and Austin 1966), as shown below,

$$\tau = \frac{6\mu Q_C}{h^2 w} = \frac{6\mu Q_T (h+t)}{0.9 \times \pi (R^2 - r^2) \times h^2} \quad (2)$$

where μ, Q_C, Q_T, and w are the viscosity of culture medium, flow rate between adjacent spacers, total flow rate through the RS, and spacing between each spacer, respectively. Calculated shear stress in a medium RS is presented in Fig. 3b.

As cells in the RS consume oxygen in the culture medium, the cells near the downstream will experience lower oxygen concentration than those near the upstream. The oxygen concentration difference between the upstream and the downstream, $\Delta[O_2]$, will be affected by the flow rate and length of the RS. Assuming a uniform oxygen uptake rate of individual cells in the RS, $\Delta[O_2]$ can be calculated as below.

$$\Delta[O_2] = \rho \times OUR_C \times \left(\frac{A}{Q_T} \right) = \rho \times OUR_C \times \frac{2\pi (R^2 - r^2) L}{Q_T (h+t)} \times 0.9 \quad (3)$$

where ρ and OUR_C are the cell density per unit area and the oxygen uptake rate of a single cell. From our experiments with RSs, the OUR_C was measured to be 105.2 pg/day/cell (or 38.04 amol/s/cell) and the typical oxygen concentration at the upstream was about 6.23 mg/L. In Fig. 3c,

$\Delta[O_2]$ in a medium RS is presented based on the cell density of 10^5 cells/cm^2. It is proportional to the length of the RS, L, and inversely proportional to the total flow rate, Q_T. The shear stress and $\Delta[O_2]$ can be easily adjusted by varying the spacer height, h, and the flow rate, Q_T, as shown in Fig. 3d.

We examined the proliferation of the CHO cells in a small RS, as shown in Fig. 4. The oxygen consumption rate was used as a primary indicator of the total metabolic activity of the cells. To this end, the dissolved oxygen concentrations at the upstream and downstream were measured, as shown in Fig. 4a. The medium was not circulated for the initial 4 hours after cell seeding to enhance cell attachment. The medium was then perfused with a peristaltic pump at a minimum flow rate of 80 μL/min, which is the minimum flow rate of the used pumping system. As the cell proliferated, the downstream oxygen concentration decreased rapidly, whereas the upstream dissolved oxygen concentration exhibited little change. Once the downstream oxygen concentration decreased below 3 mg/L, the flow rate was doubled. The morphology of the CHO cells was checked at 4, 48, and 94 hours after the cell seeding by imaging the PET film unrolled from the RS, as shown in Fig. 4b and Supplementary Fig. 1. The CHO cells were successfully attached to the PET substrate after 4 hours, with a seeding efficiency of 98%. At 48 and 94 hours, the CHO cells showed normal morphology and the cell density increased substantially. Based on the image analysis, the cell density was 4.89×10^3, 2.33×10^4, and 1.67×10^5 cells/cm^2 at 4, 48, and 94 hours after the cell seeding, respectively.

The unique configuration of the RS allowed direct measurement of the oxygen consumption rate, based on the flow rate and the difference between the upstream oxygen concentration and the downstream oxygen concentration, as shown in Fig. 4c. As mentioned before, the peristaltic pump was turned off after the cell seeding for 4 hours to ensure cell attachment. During this period, the

cells consumed the oxygen in the culture medium confined in the RS. When the perfusion started, the consumed medium passed through the downstream oxygen sensor and a peak in the oxygen consumption rate was produced. After the initial peak, the oxygen consumption rate increased exponentially, suggesting exponential proliferation of the CHO cells in the RSs. After 80 hours of active growth, the oxygen consumption rate showed a gradual saturation. The number of the CHO cells harvested from 'SRS - 2' and 'SRS - 3' in Fig. 4c were 4.37×10^7 and 3.6×10^7, respectively. The cell density was $(1.60 \pm 0.2) \times 10^5$ cells/cm^2, which was similar to the cell density in a tissue culture flask at 90% confluency. The gradual saturation of the cell proliferation can be attributed to the contact inhibition (McClatchey 2012) and the lack of the culture area for newly born cells. The total fold-increase of the CHO cells in the small RS was 32.1 ± 4.3 times and the average culture time was 94.3 ± 1.2 hours. The average doubling time was 18.85 ± 0.56 hours. Figure 4d shows the growth rate, μ (Baptista et al. 2013; Nath et al. 2017) of CHO cells in the small RS.

After successful expansion with small RSs, medium RSs with a 100 ml spinner flask with a vented cap (MRS-100ml) or a 1 L spinner flask with a vented cap (MRS-1) were tested, as shown in Fig. 5a. Both cases clearly showed exponential cell growth for over 72 hours with MRS-100ml and 96 hours with MRS-1. However, the upstream oxygen concentration dropped significantly when the oxygen consumption rate went over 8 μg/min for MRS-100ml and 40 μg/min for MRS-1, due to the limited gas transfer rate of the spinner flasks with simple vented caps.

In the third trial, denoted as 'MRS - 2', sparging was tested to increase the gas transfer rate. When the upstream oxygen concentration started to drop, the culture medium in the reservoir was sparged for 5 minutes. The upstream oxygen concentration increased very rapidly with sparging, as shown in Fig. 5b and Supplementary Fig. 2c. However, a thick layer of foam was generated quickly and prevented the rotation of the impeller. In another attempt denoted as 'MRS - 3', the chamber was

slightly pressurized to enhance the gas transfer rate. Humidified air with 5% CO_2 was injected into the 1 L spinner flask's overhead space using an air pump at 2 mL/s. When the upstream oxygen concentration eventually started to decrease with the increased oxygen consumption rate near the end of the culture, the flask was pressurized by attaching a 4 m long thin tubing with a diameter of 0.8 mm at the end of the vent. In a separate testing, the attachment of the thin tubing increased the pressure by 0.3 psi. Both the upstream and downstream oxygen concentrations increased by about 18%, as shown in Supplementary Fig. 2d. In all of these trials, the CHO cells showed active proliferation, evidenced by the exponential increase in oxygen consumption and the decrease in the glucose concentration and the pH, as shown in Fig. 5c and 5d. The average growth rate of these four trials was comparable to that of the small RSs, as shown in Fig. 5e.

Based on these trials, the pressurization approach as in 'MRS-3' was selected and the setup was further improved. To provide sufficient oxygen, humidified air with 5% CO_2 was injected into the overhead space of the spinner flask with an air pump. A rotameter was attached to the vent of the spinner flask to control the pressure of the reservoir, and a nutrient supplement was used to replenish the depleted nutrients in the culture medium. This trial was termed as 'MRS - 4' and its setup is detailed in Supplementary Fig. 3. For the initial 50 hours, the air was injected without being humidified by accident and the medium volume decreased by 100 mL, producing osmotic pressure. This osmotic pressure decreased the proliferation rate of the cells in the RS, as shown in Fig. 6a. The culture medium was fully changed at 204 hours and the cells proliferated actively afterward. At 225 hours after seeding, the upstream oxygen concentration started to decrease, as shown in Supplementary Fig. 2e. We pressurized the spinner flask by closing the valve on the rotameter. The pressure increased by 1.8 psi and the outlet air flow rate reduced from 17 mL/s to 1 mL/s. The upstream oxygen concentration was kept above 5.4 mg/L with an oxygen consumption

rate of 80 μg/min. In this trial, over 958 million CHO cells were produced from 9.1 million cells. As the volume of a medium RS was 16 mL and the surface area was 1831 cm^2, the resulting culture density was 6.0×10^7 cells/mL or 5.2×10^5 cells/cm^2.

The growth rate, μ, of the CHO cells in the RSs was 1.001 ± 0.225 day^{-1} on average, which is significantly higher than other studies. Other studies (Clincke et al. 2013; Ducommun et al. 2002; Kwon et al. 2017; Lee et al. 2005; Mignot et al. 1990; Zhang et al. 2015) that expanded CHO cells with suspension culture reported a growth rate in the range of 0.17 – 0.72 day^{-1}. We believe that low shear stress, sufficient mass transfer rate, and monolayer culture provided the optimal environments for cellular growth. Similarly, the maximum culture density of the RS, which was 6.0×10^7 cells/mL, was similar or higher than other studies summarized in Supplementary Table 1. In earlier studies, the final culture density of 12.3×10^7 cells/mL was achieved (Clincke et al. 2013) using a disposable plastic bag on a rocking platform. A density of 13.0×10^7 cells/mL was also reported (Zhang et al. 2015) based on a non-woven matrix-based bioreactor. Other than these two studies, most studies (Ducommun et al. 2002; Kwon et al. 2017; Lee et al. 2005; Mignot et al. 1990) on high-capacity CHO cell culturing reported a maximum culture density in the range of $0.1 \times 10^7 – 3.6 \times 10^7$ cells/mL.

We also cultured mESCs with a small RS. The oxygen consumption rate exhibited exponential growth, as shown in Fig. 7a. The average growth rate was lower than the CHO cells, as evidenced in Fig. 7b. The average fold increase was 4.13 ± 1.31 times and the average culture time was 95.61 ± 19.57 hours. The expanded mESC maintained strong pluripotency. As shown in Fig. 7c, the expression levels of three pluripotent genes, Nanog, Sox2, and Pou5f1 were similar between the mESCs expanded with small RSs and those cultured with standard 2D tissue culture plastic-wares.

A strong and uniform expression of Oct4 was confirmed by immunofluorescence staining the mESCs expanded with a small RS, as shown in Fig. 7d.

As demonstrated with the successful expansion of CHO cells and mESCs, the RS is an efficient platform to culture anchorage-dependent cells on a large scale. The unique geometry of the RS provides a number of advantages over conventional platforms. First, the RS can provide consistent microenvironments that are independent of its capacity, as the capacity of the RS is expanded by increasing the length of the rolled plastic film with same spacer height. As a result, the growth and metabolism of the cells are consistent with different capacities of the RSs. For instance, μ and OUR_C of CHO cells in small RSs were 1.06 ± 0.16 day^{-1} and 39.07 ± 3.72 amol/s/cell, whereas those in medium RSs were 1.00 ± 0.23 day^{-1} and 37.63 ± 3.4 amol/s/cell. As a reference, OUR_C of CHO cells were reported to be 47 – 66.8 amol/s/cell (Goudar et al. 2011) and 55 amol/s/cell (Gray et al. 1996). Second, the cells in the RS experience significantly reduced shear stress than those in other culture platforms, as nutrients and gases are transported through convection in a unidirectional laminar flow. The shear stress on the cells in this study ranges from 1.9 mPa to 61 mPa for a small RS with a flow rate of 0.08 – 2.6 mL/min, and from 4.2 mPa to 135 mPa for a medium RS with a flow rate of 1.3 – 41.6 mL/min. It should be noted that the shear stress was increased exponentially to support the exponential cell proliferation and the cells experienced the maximum shear stress only at the last day of the culture when the cells were highly confluent. The average shear stress over the culture time was 21.06 ± 3.74 mPa for a small RS and 12.08 ± 7.20 mPa for a medium RS. These values were substantially lower than the shear stress in other cell expansion platforms (Badenes et al. 2016; Wang et al. 2013; Youn et al. 2005) and the shear stress that would adversely affect the cells (Ma et al. 2002). For instance, the shear stress in a 100 ml spinner flask was reported to be 200 – 520 mPa with a pitched-blade impeller, 450 – 780 mPa with

a paddled impeller, and 152 mPa with a glass-ball impeller (Wang et al. 2013). In literatures (Abraham et al. 2017), the non-lethal but harmful effect of the shear stress was reported with a shear stress over 1 Pa. Stem cells are in general more sensitive to the shear stress (Stolberg and McCloskey 2009). It was reported that mESCs were damaged with a shear stress of 780 mPa (Cormier et al. 2006) and that differentiation and gene expression of mESC were affected with a shear stress over 1 Pa (Illi et al. 2005; McCloskey et al. 2006; Stolberg and McCloskey 2009). More importantly, the shear stress in RS is uniform, independent of the culture capacity, and readily controllable with the flow rate and the spacer's height. Third, the cells are separated from the medium reservoir and the culture medium can be agitated, sparged, or replaced without damaging or losing the cells. Lastly, the combined metabolic activity of cells in the RS can be directly measured from the oxygen concentrations at the upstream and downstream. This allows real-time evaluation of cellular conditions and facilitates optimization of culture conditions.

Oxygen is one of the most limited components in the culture medium due to its low solubility. In this paper, we increased the flow rate to maintain the downstream oxygen concentration above 3 mg/L, whereas the upstream oxygen concentration was about 6.5 mg/L. The variation of the oxygen concentration in the RS may result in heterogeneity of expanded cells or a non-optimal level of cell proliferation. The gradient of the oxygen concentration in the RS can be reduced by increasing the flow rate of the culture medium or the spacer's height at the cost of increased shear stress or reduced culture density, as illustrated in Fig. 3. For instance, if we increase the spacer's height by 50% while fixing the shear stress, the surface area, and the RS length, then $\Delta[O_2]$ will decrease by 55.6% with a flow rate increase of 125%.

In this study, the RS setup was operated manually and frequent human interventions could cause human error or contamination. For instance, manual collection of samples for pH and glucose

measurement leave a brief spike on oxygen concentration measurement, as shown in supplementary Fig. 2. Fortunately, the configuration of the RS bioreactor is inherently easy to automate. In the future work, we are planning to automate the RS bioreactor, implementing automatic control systems for controlling the flow rate by monitoring the downstream oxygen concentration and maintaining pH by integrating in-line pH sensors and a syringe pump loaded with acid neutralizer.

Conclusion

A reliable and efficient platform to culture mammalian cells on a large scale is essential in advanced biomanufacturing. In this paper, we present the RS as a novel platform for high-density adherent culture of mammalian cells and demonstrate the expansion of CHO cells and mESCs. The RS provides high surface-area-to-volume ratio and the cells growing in the RS experience significantly lower shear stress than other platforms. Moreover, the microenvironment in the RS is fully defined and various aspects of the RS can be precisely tailored for specific applications. The RS will provide a scalable and robust platform to culture recombinant cells for biopharmaceutics as well as shear-sensitive stem cells for tissue engineering.

Conflicts of interest: A patent application has been filed on this technology by Louisiana State University.

Acknowledgements: The ES cell line used for this research project, E14 RP11-88L12 NKX2-5-EmGFP ES cell line, RRID:MMRRC_030473-UCD, was obtained from the Mutant Mouse Resource & Research Centers, a NCRR-NIH funded strain repository, and was donated to the

MMRRC by Dr. Bruce Conklin, M.D., Gladstone Institute of Cardiovascular Disease. A. Mehrnezhad was supported from the Louisiana Board of Regents (Grant LEQSF(2014-17)-RD-A-05) and Katie M. Hamel was supported by the Flagship Graduate Fellowship.

Author contributions: K.P. conceived RS and RS-bioreactor; K.P., A.Y., and A.M. built experimental setups; A.Y. collected data on RS culture; K.P., A.Y., and J.P.J. designed experiments; J.P.J. and K.M.H. provided and characterized mESCs.

Reference

Abraham E, Ahmadian BB, Holderness K, Levinson Y, McAfee E (2017) Platforms for Manufacturing Allogeneic, Autologous and iPSC Cell Therapy Products: An Industry Perspective. In: New Bioprocessing Strategies: Development and Manufacturing of Recombinant Antibodies and Proteins, vol 165. Springer, Cham, pp 323-350. doi:https://doi.org/10.1007/10_2017_14

Abu-Reesh I, Kargi F Biological responses of hybridoma cells to hydrodynamic shear in an agitated bioreactor Enzyme and microbial technology 13:913-919 (1991)

Amit M et al. Suspension culture of undifferentiated human embryonic and induced pluripotent stem cells Stem Cell Reviews and Reports 6:248-259 (2010)

Badenes SM et al. Defined Essential 8™ Medium and Vitronectin Efficiently Support Scalable Xeno-Free Expansion of Human Induced Pluripotent Stem Cells in Stirred Microcarrier Culture Systems PloS one 11:e0151264 (2016)

Baptista RP, Fluri DA, Zandstra PW High density continuous production of murine pluripotent cells in an acoustic perfused bioreactor at different oxygen concentrations Biotechnology and bioengineering 110:648-655 (2013)

Barbulovic-Nad I, Au SH, Wheeler AR A microfluidic platform for complete mammalian cell culture Lab on a Chip 10:1536-1542 (2010)

Billiet T, Gevaert E, De Schryver T, Cornelissen M, Dubruel P The 3D printing of gelatin methacrylamide cell-laden tissue-engineered constructs with high cell viability Biomaterials 35:49-62 (2014)

Chen A, Ting S, Seow J, Reuveny S, Oh S Considerations in designing systems for large scale production of human cardiomyocytes from pluripotent stem cells Stem cell research & therapy 5:12 (2014)

Chong JJ et al. Human embryonic-stem-cell-derived cardiomyocytes regenerate non-human primate hearts Nature 510:273 (2014)

Chotteau V, Zhang Y, Clincke M-F Very High Cell Density in Perfusion of CHO Cells by ATF, TFF, Wave Bioreactor, and/or CellTank Technologies–Impact of Cell Density and Applications Continuous Processing in Pharmaceutical Manufacturing (2014)

Chu L, Robinson DK Industrial choices for protein production by large-scale cell culture Current opinion in biotechnology 12:180-187 (2001)

Cino J, Mirro R, Kedzierski S An update in the advantages of Fibra-Cel disks for cell culture Appl Note Eppendorf Google Scholar (2003)

Clincke MF, Mölleryd C, Zhang Y, Lindskog E, Walsh K, Chotteau V Very high density of CHO cells in perfusion by ATF or TFF in WAVE bioreactor™. Part I. Effect of the cell density on the process Biotechnology progress 29:754-767 (2013)

Cormier JT, Nieden NIZ, Rancourt DE, Kallos MS Expansion of undifferentiated murine embryonic stem cells as aggregates in suspension culture bioreactors Tissue engineering 12:3233-3245 (2006)

Ducommun P, Ruffieux PA, Kadouri A, Von Stockar U, Marison I Monitoring of temperature effects on animal cell metabolism in a packed bed process Biotechnology and bioengineering 77:838-842 (2002)

Eibl R, Werner S, Eibl D (2009) Bag bioreactor based on wave-induced motion: characteristics and applications. In: Disposable bioreactors. Springer, pp 55-87

Gareau T, Lara GG, Shepherd RD, Krawetz R, Rancourt DE, Rinker KD, Kallos MS Shear stress influences the pluripotency of murine embryonic stem cells in stirred suspension bioreactors Journal of tissue engineering and regenerative medicine 8:268-278 (2014)

Goudar CT, Piret JM, Konstantinov KB Estimating cell specific oxygen uptake and carbon dioxide production rates for mammalian cells in perfusion culture Biotechnology progress 27:1347-1357 (2011)
Gray DR, Chen S, Howarth W, Inlow D, Maiorella BL CO 2 in large-scale and high-density CHO cell perfusion culture Cytotechnology 22:65-78 (1996)
Gupta P, Ismadi M-Z, Verma PJ, Fouras A, Jadhav S, Bellare J, Hourigan K Optimization of agitation speed in spinner flask for microcarrier structural integrity and expansion of induced pluripotent stem cells Cytotechnology 68:45-59 (2016)
Holt JK et al. Fast mass transport through sub-2-nanometer carbon nanotubes Science 312:1034-1037 (2006)
Illi B et al. Epigenetic histone modification and cardiovascular lineage programming in mouse embryonic stem cells exposed to laminar shear stress Circulation research 96:501-508 (2005)
Jaccard N, Griffin LD, Keser A, Macown RJ, Super A, Veraitch FS, Szita N Automated method for the rapid and precise estimation of adherent cell culture characteristics from phase contrast microscopy images Biotechnology and bioengineering 111:504-517 (2014)
Jenkins MJ, Farid SS Human pluripotent stem cell-derived products: Advances towards robust, scalable and cost-effective manufacturing strategies Biotechnology journal 10:83-95 (2015)
Kohlmeier F, Maya-Mendoza A, Jackson DA EdU induces DNA damage response and cell death in mESC in culture Chromosome research 21:87-100 (2013)
Krawetz R, Taiani JT, Liu S, Meng G, Li X, Kallos MS, Rancourt DE Large-scale expansion of pluripotent human embryonic stem cells in stirred-suspension bioreactors Tissue Engineering Part C: Methods 16:573-582 (2009)
Kwon T, Prentice H, De Oliveira J, Madziva N, Warkiani ME, Hamel J-FP, Han J Microfluidic Cell Retention Device for Perfusion of Mammalian Suspension Culture Scientific reports 7:6703 (2017)
Lee JC, Chang HN, Oh DJ Recombinant antibody production by perfusion cultures of rCHO cells in a depth filter perfusion system Biotechnology progress 21:134-139 (2005)
Leung HW, Chen A, Choo AB, Reuveny S, Oh SK Agitation can induce differentiation of human pluripotent stem cells in microcarrier cultures Tissue Engineering Part C: Methods 17:165-172 (2010)
Longuet-Higgins H, Austin G The kinetics of osmotic transport through pores of molecular dimensions Biophysical journal 6:217-224 (1966)
Ma N, Koelling KW, Chalmers JJ Fabrication and use of a transient contractional flow device to quantify the sensitivity of mammalian and insect cells to hydrodynamic forces Biotechnology and bioengineering 80:428-437 (2002)
McClatchey AI Contact inhibition (of proliferation) redux Current opinion in cell biology 24:685-694 (2012)
McCloskey KE, Smith DA, Jo H, Nerem RM Embryonic stem cell-derived endothelial cells may lack complete functional maturation in vitro Journal of vascular research 43:411-421 (2006)
Merten OW et al. Comparison of different bioreactor systems for the production of high titer retroviral vectors Biotechnology progress 17:326-335 (2001)
Mignot G, Faure T, Ganne V, Arbeille B, Pavirani A, Romet-Lemonne J Production of recombinant Von Willebrand factor by CHO cells cultured in macroporous microcarriers Cytotechnology 4:163-171 (1990)
Mizukami A et al. A Fully-Closed and Automated Hollow Fiber Bioreactor for Clinical-Grade Manufacturing of Human Mesenchymal Stem/Stromal Cells Stem Cell Reviews and Reports 14:141-143 (2018)

Moreira JL, Santana PC, Feliciano AS, Cruz PE, Racher AJ, Griffiths JB, Carrondo MJ Effect of viscosity upon hydrodynamically controlled natural aggregates of animal cells grown in stirred vessels Biotechnology progress 11:575-583 (1995)
Nath SC, Nagamori E, Horie M, Kino-oka M Culture medium refinement by dialysis for the expansion of human induced pluripotent stem cells in suspension culture Bioprocess and biosystems engineering 40:123-131 (2017)
Oh S, Nienow A, Al-Rubeai M, Emery A The effects of agitation intensity with and without continuous sparging on the growth and antibody production of hybridoma cells Journal of biotechnology 12:45-61 (1989)
Olmer R et al. Long term expansion of undifferentiated human iPS and ES cells in suspension culture using a defined medium Stem cell research 5:51-64 (2010)
Reichert JM, Rosensweig CJ, Faden LB, Dewitz MC Monoclonal antibody successes in the clinic Nature biotechnology 23:1073 (2005)
Sen A, Kallos MS, Behie LA Expansion of mammalian neural stem cells in bioreactors: effect of power input and medium viscosity Developmental Brain Research 134:103-113 (2002)
Senger RS, Karim MN Effect of Shear Stress on Intrinsic CHO Culture State and Glycosylation of Recombinant Tissue-Type Plasminogen Activator Protein Biotechnology progress 19:1199-1209 (2003)
Shiba Y et al. Allogeneic transplantation of iPS cell-derived cardiomyocytes regenerates primate hearts Nature 538:388 (2016)
Sinacore MS, Drapeau D, Adamson S Adaptation of mammalian cells to growth in serum-free media Molecular biotechnology 15:249-257 (2000)
Singh V Disposable bioreactor for cell culture using wave-induced agitation Cytotechnology 30:149-158 (1999)
Stoelzle S et al. Automated patch clamp on mESC-derived cardiomyocytes for cardiotoxicity prediction Journal of biomolecular screening 16:910-916 (2011)
Stolberg S, McCloskey KE Can shear stress direct stem cell fate? Biotechnology progress 25:10-19 (2009)
Walsh G Biopharmaceutical benchmarks 2014 Nature biotechnology 32:992 (2014)
Wang Y, Chou B-K, Dowey S, He C, Gerecht S, Cheng L Scalable expansion of human induced pluripotent stem cells in the defined xeno-free E8 medium under adherent and suspension culture conditions Stem cell research 11:1103-1116 (2013)
Wolf CB, Mofrad MR (2009) Mechanotransduction and its role in stem cell biology. In: Trends in stem cell biology and technology. Springer, pp 389-403
Wurm FM Production of recombinant protein therapeutics in cultivated mammalian cells Nature biotechnology 22:1393 (2004)
Yan Y et al. Fabrication of viable tissue-engineered constructs with 3D cell-assembly technique Biomaterials 26:5864-5871 (2005)
Youn BS et al. Large-Scale Expansion of Mammary Epithelial Stem Cell Aggregates in Suspension Bioreactors Biotechnology progress 21:984-993 (2005)
Zhang Y, Stobbe P, Silvander CO, Chotteau V Very high cell density perfusion of CHO cells anchored in a non-woven matrix-based bioreactor Journal of biotechnology 213:28-41 (2015)

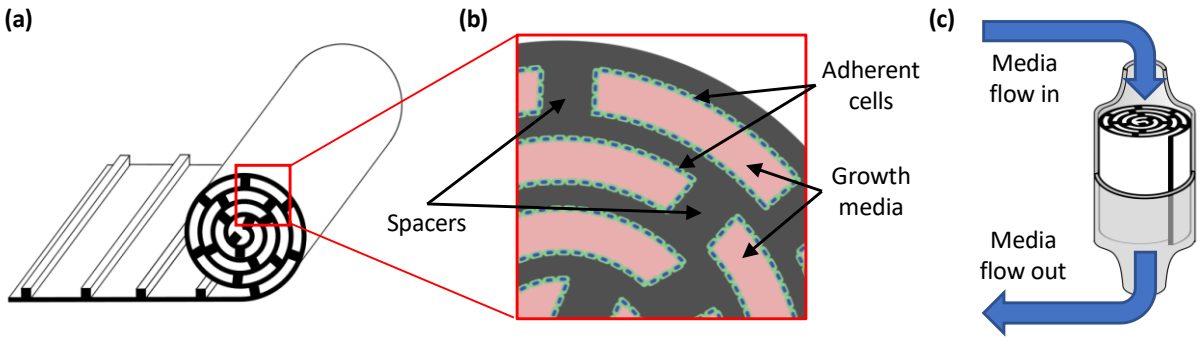

Fig. 1 Schematic diagram of rolled scaffold (RS). (a) RS is made from PET film with repeating spacers. The film is rolled to form a cylindrical shape with numerous channels. (b) The spacers on the PET film ensure a uniform gap between the layers. The cells are cultured on the inner surface. (c) RS is placed in a holder and the culture medium flows through the gaps

Fig. 1 Schematic diagram of rolled scaffold (RS). (a) RS is made from PET film with repeating spacers. The film is rolled to form a cylindrical shape with numerous channels. (b) The spacers on the PET film ensure a uniform gap between the layers. The cells are cultured on the inner surface. (c) RS is placed in a holder and the culture medium flows through the gaps

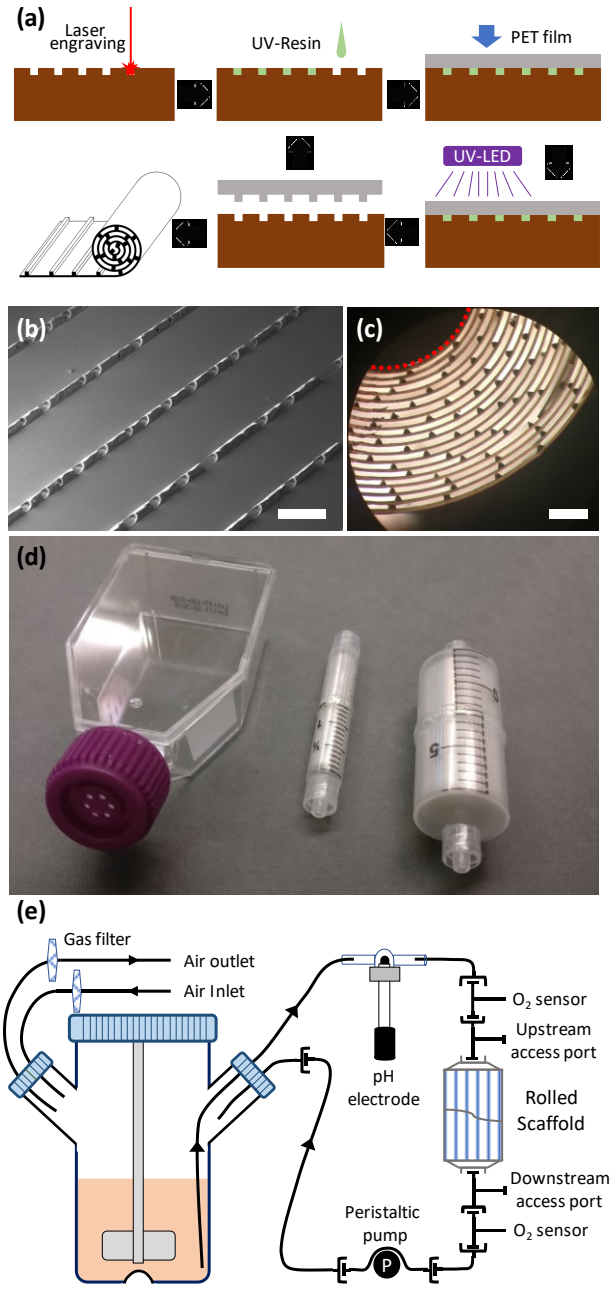

Fig. 2 Fabrication process and experimental setup of RS. (a) Fabrication process of RS is presented. (b) SEM image of a flat PET film with spacers. Scale bar is 600 µm. (c) Optical image of RS from side view. Scale bar is 700 µm. (The dotted line shows the core rod.) (d) A medium RS (1831 cm^2) and a small RS (251 cm^2) are shown with a T-25 flask. (e) Experimental setup and fluidic connection of RS-based bioreactor

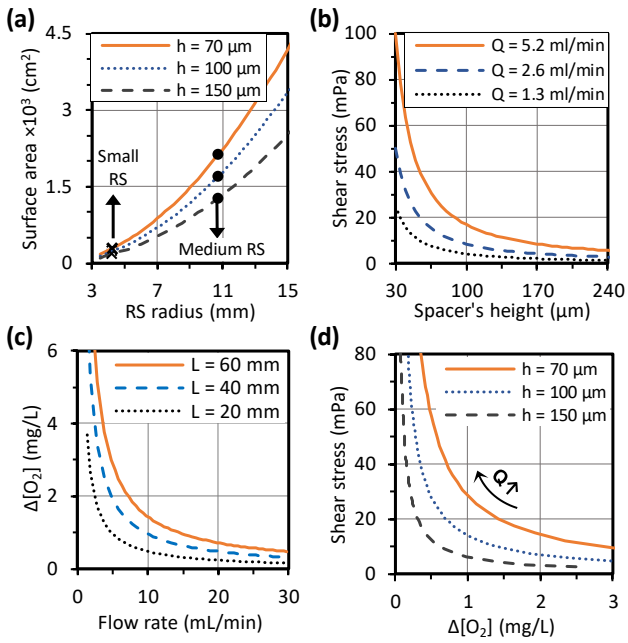

Fig. 3 Dimensions and operational parameters of RS. (a) The surface area, A, is proportional to the square of the radius, R, and the inverse of the spacer's height, h. (b) The shear stress can be decreased by increasing h or decreasing the flow rate, Q_T. (c) The oxygen concentration difference between upstream and downstream, $\Delta[O_2]$, can be controlled with Q_T or the length of the RS, L. (d) The shear stress, τ, and $\Delta[O_2]$ depend on the flowrate and the gap between layers

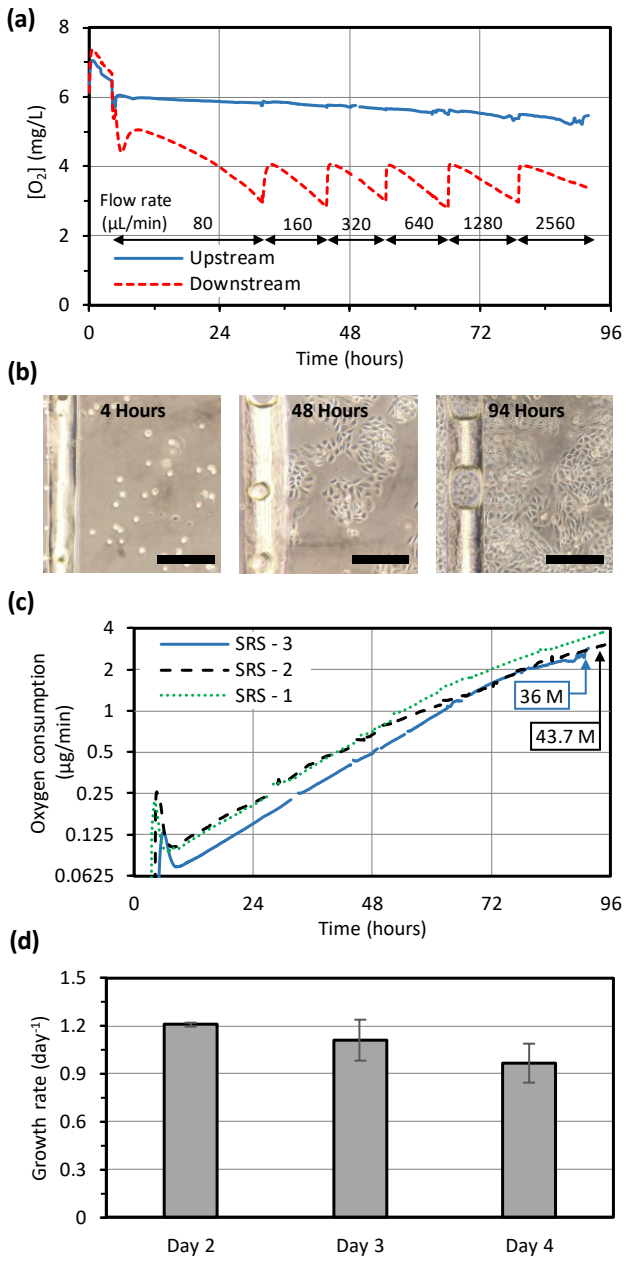

Fig. 4 Expansion of CHO cells with a small RS. (a) Dissolved oxygen concentration at upstream and downstream was measured over 90 hours. The flow rate was doubled when the downstream oxygen concentration became below 3 mg/L. (b) Phase-contrast images of CHO cells on an unrolled small RS shows active proliferation. Scale bars are 150 µm. (c) The oxygen consumption increased exponentially. The numbers of harvested CHO cells after expansion are shown in boxes. (d) Growth rate of CHO cells

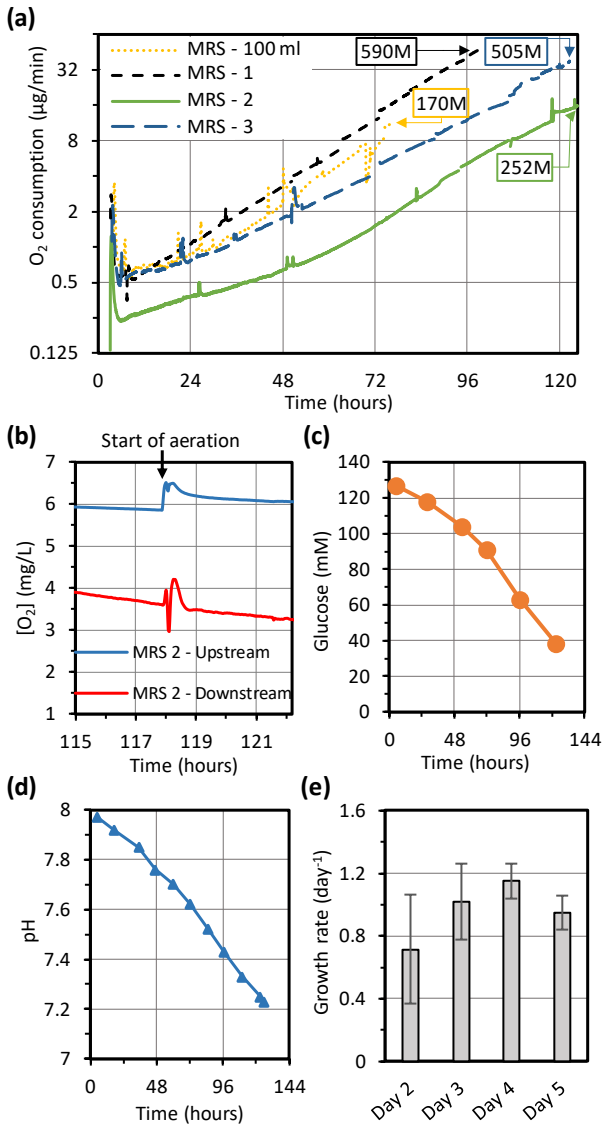

Fig. 5 Expansion of CHO cells with a medium RS. (a) The oxygen consumption increased exponentially. The numbers of harvested CHO cells after expansion are shown in boxes. (b) Dissolved oxygen concentrations at upstream and downstream increased immediately when the reservoir was sparged. (c) The glucose concentration decreased throughout the cell expansion, while (d) pH slightly decreased in that duration (MRS–2). (e) The cells showed active proliferation

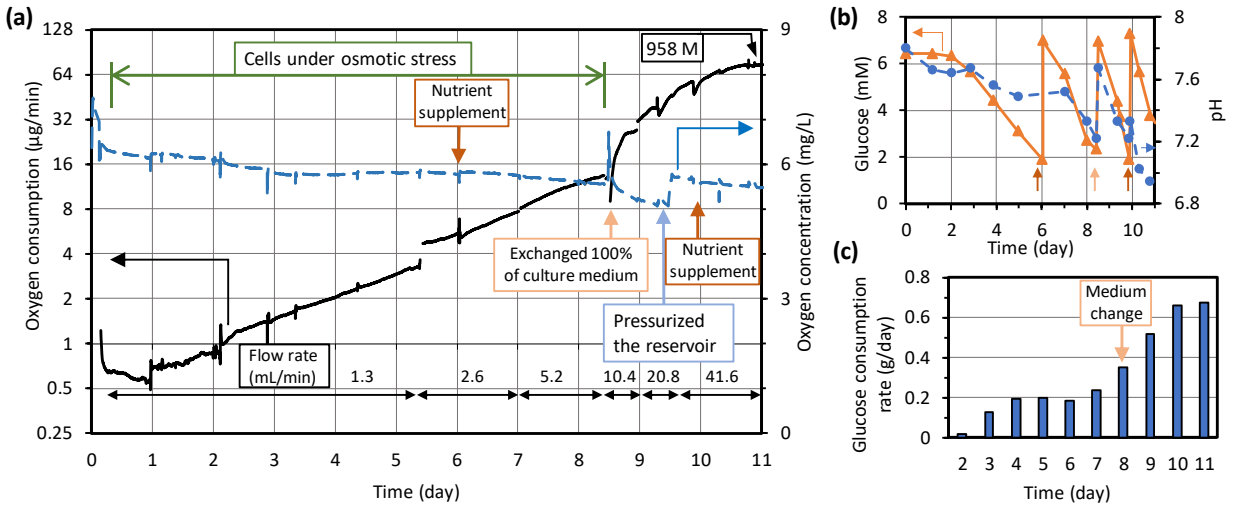

Fig. 6 CHO expansion in a medium RS with pressurization. (a) By pressurizing the reservoir, near 1 billions of CHO cells were successfully harvested. About 100 ml of the culture medium was evaporated during initial 50 hours. The osmotic stress reduced the proliferation, but the cells fully recovered after the medium change. (b) Glucose and pH of the medium in the reservoir was monitored daily. To provide sufficient nutrients, 28mL of nutrient supplement was added on day 6 and 10. The culture medium was exchanged on day 8. (c) The glucose consumption rate increased significantly after the culture medium was changed

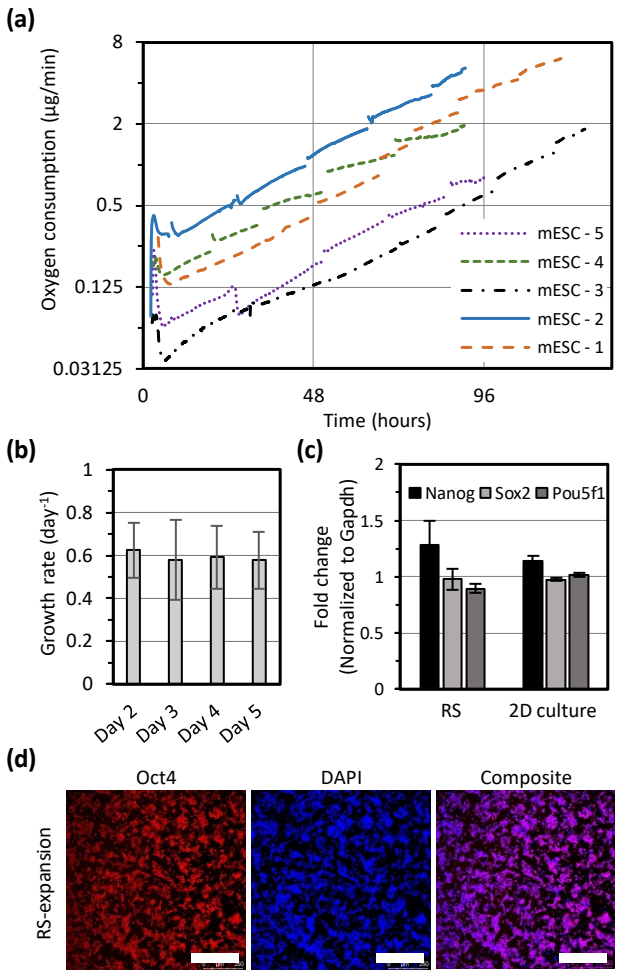

Fig. 7 mESC expansion in a small RS. (a) The oxygen consumption of mESC increased exponentially. (b) mESC growth rate in the RS over time. (c) Relative pluripotent gene expression normalized to Gapdh at the end of mESC expansion in a small RS. (d) Immunofluorescence staining of Oct4 in RS-expanded mESCs. Scale bars are 300 µm.

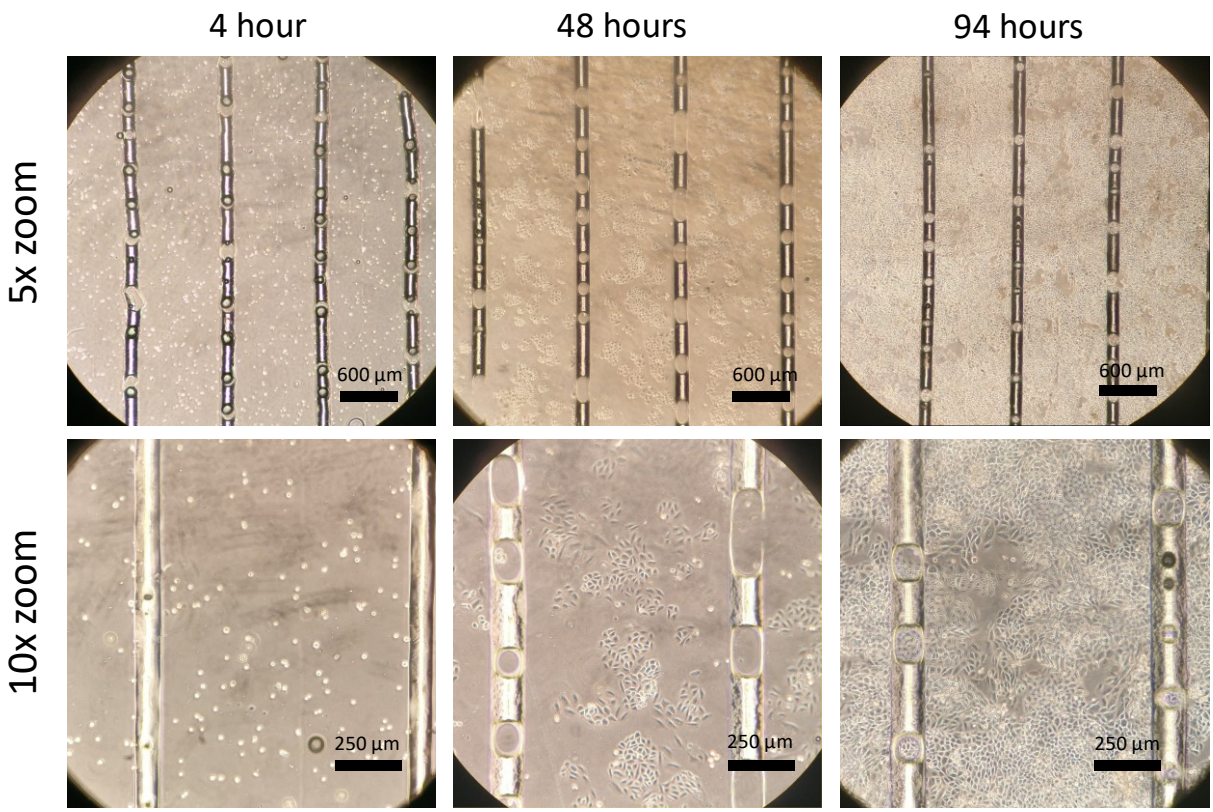

Supplementary Fig. 1 Phase-contrast images of CHO cells on an unrolled small RS taken at 4, 48, and 94 hours after cell seeding

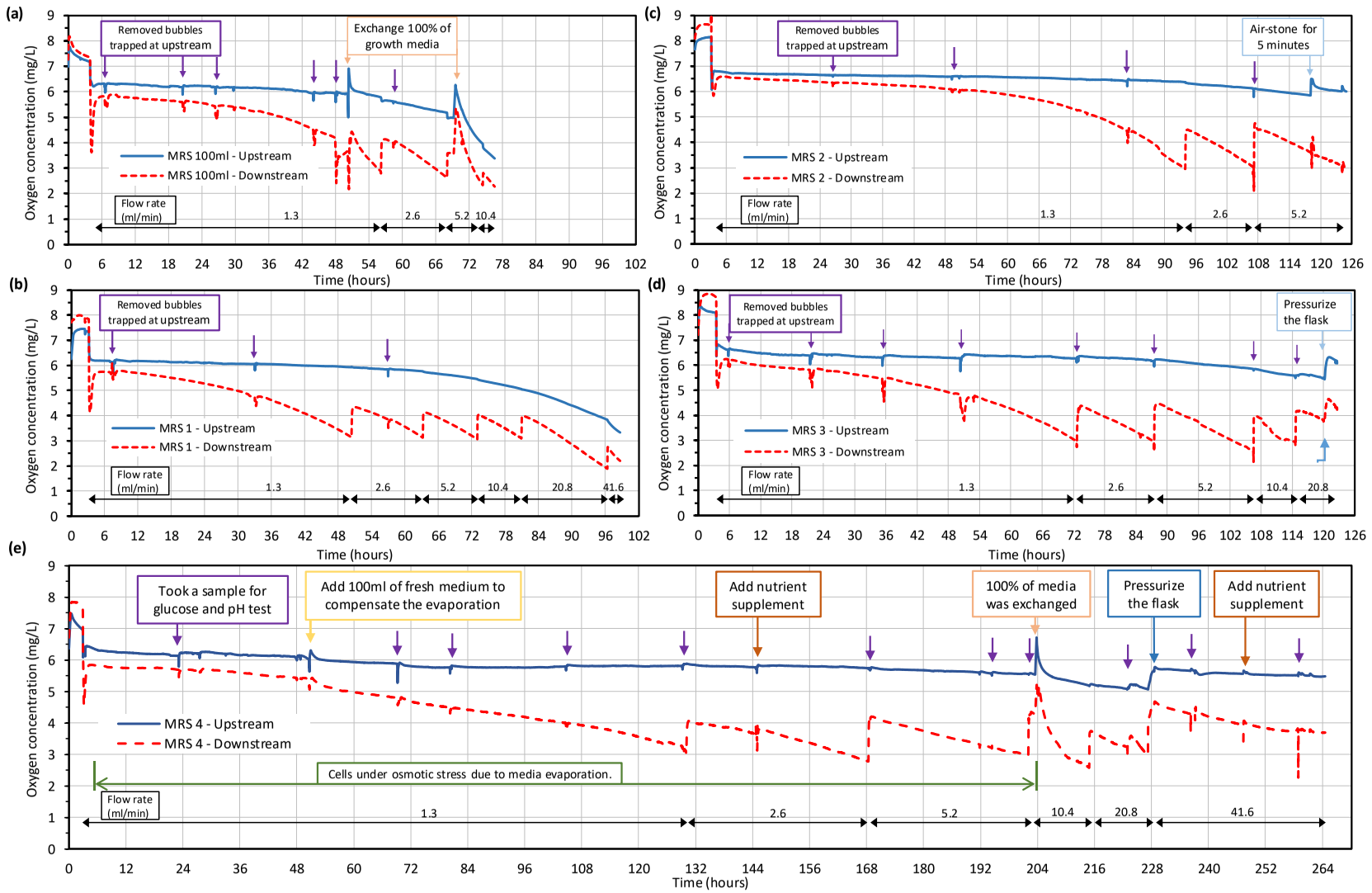

Supplementary Fig. 2 Oxygen concentration at upstream and downstream for (a) MRS – 100ml, (b) MRS – 1, (c) MRS – 2, (d) MRS – 3, and (e) MRS – 4

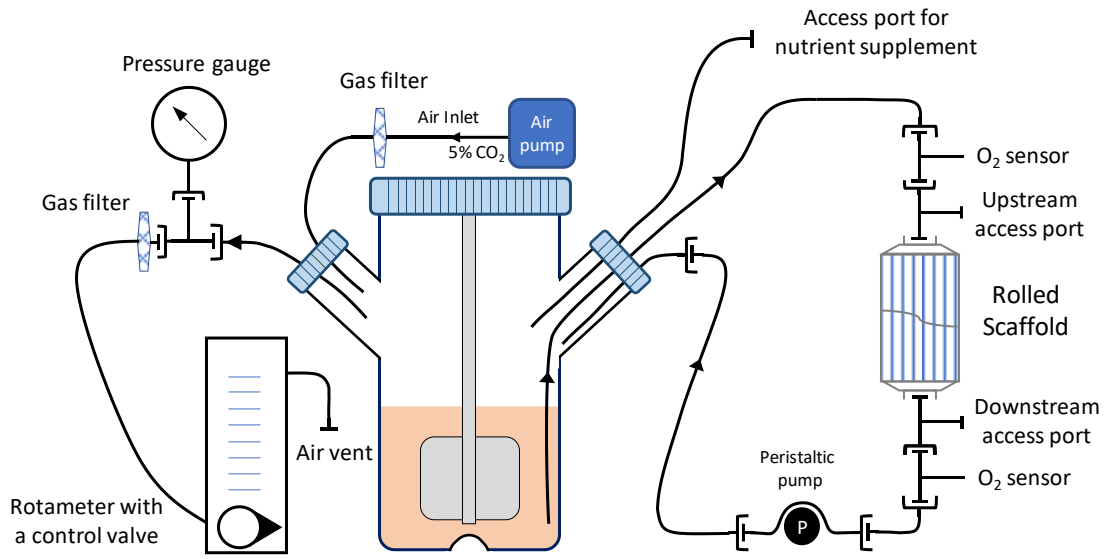

Supplementary Fig. 3 Experimental setup for MRS – 4. By using a rotameter, the pressure of the bioreactor was controlled

~~**Fig. 2** Fabrication process and experimental setup of RS. (a) Fabrication process of RS is presented. (b) SEM image of a flat PET film with spacers. Scale bar is 600 μm. (c) Optical image of RS from side view. Scale bar is 700 μm. (The dotted line shows the core rod.) (d) A medium RS (1831 cm^2) and a small RS (251 cm^2) are shown with a T-25 flask. (e) Experimental setup and fluidic connection of RS-based bioreactor~~

~~**Fig. 3** Dimensions and operational parameters of RS. (a) The surface area, A, is proportional to the square of the radius, R, and the inverse of the spacer's height, h. (b) The shear stress can be decreased by increasing h or decreasing the flow rate, Q_T. (c) The oxygen concentration difference between upstream and downstream, $\Delta[O_2]$, can be controlled with Q_T or the length of the RS, L. (d) The shear stress, τ, and $\Delta[O_2]$ depend on the flowrate and the gap between layers~~

Fig. 4 Expansion of CHO cells with a small RS. (a) Dissolved oxygen concentration at upstream and downstream was measured over 90 hours. The flow rate was doubled when the downstream oxygen concentration became below 3 mg/L. (b) Phase-contrast images of CHO cells on an unrolled small RS shows active proliferation. Scale bars are 150 µm. (c) The oxygen consumption increased exponentially. The numbers of harvested CHO cells after expansion are shown in boxes. (d) Growth rate of CHO cells

Fig. 5 Expansion of CHO cells with a medium RS. (a) The oxygen consumption increased exponentially. The numbers of harvested CHO cells after expansion are shown in boxes. (b) Dissolved oxygen concentrations at upstream and downstream increased immediately when the reservoir was sparged. (c) The glucose concentration decreased throughout the cell expansion, while (d) pH level slightly decreased in that duration (MRS 2). (e) The cells showed active proliferation

Fig. 6 CHO expansion in a medium RS with pressurization. (a) By pressurizing the reservoir, near 1 billion of CHO cells were successfully harvested. About 100 ml of the culture medium was evaporated during initial 50 hours. The osmotic stress reduced the proliferation, but the cells fully recovered after the medium change. (b) Glucose and pH of the medium in the reservoir was monitored daily. To provide sufficient nutrients, 28mL of nutrient supplement was added on day 6 and 10. The culture medium was exchanged on day 8. (c) The glucose consumption rate increased significantly after the culture medium was changed

Fig. 7 mESC expansion in a small RS. (a) The oxygen consumption of mESC increased exponentially. (b) mESC growth rate in the RS over time. (c) Relative pluripotent gene expression normalized to Gapdh at the end of mESC expansion in a small RS. (d) Immunofluorescence staining of Oct4 in RS-expanded mESCs. Scale bars are 300 μm